Magnetic form factor of terbium in $Tb(OH)_3$†

T. O. Brun and G. H. Lander
Argonne National Laboratory, Argonne, Illinois 60439
(Received 28 June 1973; revised manuscript received 14 December 1973)

The magnetic form factor of terbium in $Tb(OH)_3$ has been measured from single crystals with polarized neutrons in both the paramagnetic (90 °K) and ferromagnetic (2.6 °K) states. The atomic parameters of the crystal structure were obtained from a refinement of Bragg intensities measured with unpolarized neutrons, and are in agreement with the parameters determined for other rare-earth hydroxides. This refinement indicated severe extinction effects, but corrections to both the unpolarized and polarized data were applied successfully with the simple Zachariasen formula, and with the same extinction parameter in each case. After correcting for extinction the experimental results essentially fall on a smooth curve as a function of $\sin\theta/\lambda$. At both temperatures the best fit to the experimental smooth curve is with a magnetic form factor intermediate between that derived from the nonrelativistic wave functions of Freeman and Watson, and that found experimentally for terbium metal. However, the experimental form factor is in good agreement with recent relativistic mixed-configuration Dirac-Fock wave functions calculated by Desclaux and Freeman. An examination of certain Bragg reflections that have no contribution from the terbium atom shows that the magnitude of the net spin transferred to the ligand sites is less than $0.01\mu_B$ in the ferromagnetic state when the terbium moment is $8.90\mu_B$/Tb atom.

I. INTRODUCTION

Experiments with polarized neutrons on the rare-earth metals gadolinium,[1] terbium,[2,3] and thulium[4] have shown that the spatial extent of the $4f$ electrons is more expanded in real space than indicated by theoretical nonrelativistic Hartree-Fock (HF) wave functions.[5] Moon *et al.*[1] also reported measurements on a polycrystalline sample of the ionic Gd_2O_3, in which the magnetic form factor appeared to be in good agreement with the nonrelativistic calculations. For gadolinium, however, recent relativistic calculations by Freeman and Desclaux[6] have shown that the *metal* form factor is in good agreement with theory, and it is the results for the ionic compound that are surprising and perhaps indicate covalency. The theoretical situation in gadolinium is, of course, greatly simplified by the absence of any orbital magnetic moment, but experiments on gadolinium, or its compounds, require the procurement of special isotopes because of the extremely high neutron absorption of natural gadolinium. In an effort to investigate the effects of varying environments on the spatial extent of the magnetic $4f$ electrons, we have recently reported measurements on the metallic compound TmSb.[7] The magnetic form factor of thulium was found to be in better agreement with the thulium-metal form factor than with the nonrelativistic HF calculations.[5] No single-crystal measurements of this type have been reported on truly ionic rare-earth compounds.

The present experiments on $Tb(OH)_3$ were undertaken to compare the magnetic form factor of the terbium ion with that found in terbium metal.[2,3] The hydroxide was selected because the crystal structure and magnetic properties are well known, and single crystals were available. An additional aim of the experiment was to search for any transferred spin component centered at the oxygen site, i.e., covalency effects. In Sec. II we discuss the magnetic properties of $Tb(OH)_3$, and the magnetic form factor expected on the basis of applying the tensor-operator technique. The experimental results are given in Sec. III, together with a brief discussion of the extinction effects as observed in the single crystal of $Tb(OH)_3$. A paper describing this aspect of the problem in more detail has been published. The experimental form factors are analyzed in terms of the $4f$ wave functions in Sec. IV, followed by the conclusions in Sec. V.

II. THEORY

The magnetic properties of $Tb(OH)_3$ have been investigated in detail by Wolf and his co-workers.[8-12] The compound orders ferromagnetically at (3.72 ± 0.01)°K with an ordered moment, parallel to the c axis of the hexagonal structure, of almost $9\mu_B$ per Tb atom. The magnetic properties have been explained by a detailed crystal-field analysis of optical measurements.[9] The two lowest-lying eigenstates are almost degenerate (separated by less than 0.5 cm^{-1}) and form an effective doublet. The wave functions are $0.707|6\rangle + 0.004|0\rangle + 0.707 \times |-6\rangle$, and $0.707|6\rangle - 0.707|-6\rangle$ with the c axis the axis of quantization. The next eigenstate has an energy 118 cm^{-1} (173 °K) above this doublet and may be neglected in considering the low-temperature properties. Using the crystal-field parameters given by Scott,[11] we have calculated the eigenstates and eigenvectors of the system with applied

fields up to 20 kOe and with temperatures up to 90 °K. As expected, at all temperatures and fields within this range, the induced moment arises solely from the $|\pm 6\rangle$ doublet. At 90 °K with a magnetic field of 12 kOe applied parallel to the c axis, the calculation gives an induced magnetic moment of $0.645\mu_B$ per Tb atom, and this is proportional to the applied field for $H < 20$ kOe. As discussed by Scott and Wolf,[9] the total magnetic field seen by the terbium atoms must include the magnetic dipole interactions and any nondipolar terms. These contributions are proportional to the magnetic moment at the terbium site and, in the ordered state with $9\mu_B$ per Tb atom, are 9.8 and −2.0 kOe, respectively.[9,10] The demagnetizing field at the sample position is also proportional to the moment and, from shape considerations, is estimated as −2.0 kOe in the ordered state. Including all terms gives

$$H_{\text{tot}} = H_{\text{appl}} + H_{\text{dip}} + H_{\text{nondip}} + H_{\text{demag}}$$
$$= H_{\text{appl}} + \tfrac{1}{9}(9.8 - 2.0 - 2.0)\mu \ ,$$

where μ is the moment per terbium atom in Bohr magnetons. At 90 °K and $H_{\text{appl}} < 20$ kOe the magnetic moment is proportional to the applied field and

$$H_{\text{tot}} = 1.036 H_{\text{appl}} \ . \qquad (1)$$

At temperatures below the ordering temperature of 3.72 °K, the effective $g_{\parallel}$ value[8] of 17.8 ± 0.1 implies a magnetic moment of $(8.90 \pm 0.05)\mu_B$ per Tb atom parallel to the c axis.

A rigorous calculation of the magnetic form factor of the terbium atom in $Tb(OH)_3$ must include the effects of the crystal-field interactions and the applied magnetic field. We have recently reported such calculations in a polarized-neutron study of TmSb.[7] However, these computations are unnecessary in $Tb(OH)_3$ because, as already noted, the magnetic moment arises solely from the $|\pm 6\rangle$ doublet. At temperatures small compared to the crystal-field splitting of 173 °K, the expression for the magnetic form factor is identical to that of terbium metal in its fully ordered state. Following Lovesey and Rimmer[13] [Eq. (8.19)], the magnetic form factor for reflections in the plane perpendicular to the moment direction, i.e., reflections in the (00.1) plane in this study, is

$$f(\kappa) = \langle j_0 \rangle + \tfrac{10}{27}\langle j_2 \rangle - \tfrac{1}{12}\langle j_4 \rangle + \tfrac{5}{432}\langle j_6 \rangle \ , \qquad (2)$$

where κ is the magnitude of the scattering vector $\vec{\kappa}$, and $\langle j_i \rangle$ are the radial integrals discussed in Sec. IV. If the ground-state wave functions are characterized by a single J_z state, the form factor in the plane perpendicular to the moment direction is independent of the orientation of the scattering vector. As a result, we expect a smooth form factor as a function of $\sin\theta/\lambda$. For most rare-earth ions the form factors in the ordered and paramagnetic states are different.[14] Tripositive terbium with $S = L = 3$, however, is an exception, in that the coefficient of $\langle j_2 \rangle$ is independent of the J_z state. The coefficient of $\langle j_2 \rangle$ is therefore the same at 90 °K as in the ordered state, but the numerical values of the coefficients of $\langle j_4 \rangle$ and $\langle j_6 \rangle$ are slightly decreased. In the present experiment the measurements do not extend beyond $\sin\theta/\lambda = 0.52$ Å^{-1} and for these low angles the terms in $\langle j_4 \rangle$ and $\langle j_6 \rangle$ are negligible.

III. EXPERIMENTAL DETAILS AND RESULTS

All experiments in the present study have been performed on the same single crystal of $Tb(OH)_3$, kindly lent to us by W. P. Wolf of Yale University. The preparation of these crystals is described by Mroczkowski *et al.*[15] The crystal was approximately circular in cross section (diameter 1.5 mm) and of length 4.5 mm. The c axis was parallel to the long axis of the crystal.

To characterize the sample and check the structural parameters, the integrated intensities of 531 Bragg reflections were measured at room temperature with a conventional four-circle neutron diffractometer located at the CP-5 research reactor. The incident-neutron wavelength was 1.05 Å, and one-half of reciprocal space with $\sin\theta/\lambda \leq 0.65$ Å^{-1} was examined. After averaging and correcting for absorption, 93 inequivalent reflections were obtained and used to refine the atomic structure. The coherent-scattering amplitudes used were $b_{\text{Tb}} = 0.76$, $b_0 = 0.58$, and $b_{\text{H}} = -0.374$ (all in units of 10^{-12} cm).

The polarized-neutron experiments on $Tb(OH)_3$ were performed at the CP-5 research reactor with the sample at both 90 and 2.6 °K. With this technique the ratio between Bragg intensities measured with neutrons in the two spin states is measured. This ratio R, the so-called flipping ratio, depends on the magnetic and nuclear structure factors of the Bragg reflection, M and N, respectively, as well as on instrumental and extinction corrections. If the latter are known, the ratio M/N can be determined from R. A knowledge of the crystal structure, and hence N, allows the magnetic-scattering amplitude to be found. Throughout the experiment a magnetic field of ~12 kOe was applied parallel to the c axis of the sample. From Hall-probe measurements and previous experiments, we estimate the magnitude of the applied field as 12.0 ± 0.5 kOe. For $T > 20$ °K, the temperature of the sample was measured with a calibrated platinum resistor, and temperature control to ±0.2 °K was maintained with an exchange gas system. For the low-temperature experiments, we pumped on the main helium reservoir and liquefied helium in the exchange gas chamber. The sample tempera-

ture was measured with a carbon resistance, as well as by monitoring the helium pressure in the chamber and varied between 2.4 and 2.8 °K. The incident-neutron polarization and spin-flipping efficiency were both 0.992 ± 0.003. Since both these instrumental parameters differ from the ideal value of unity, corrections must be applied to the observed flipping ratio. These corrections, normally less than 2%, have been made throughout. Other sources of possible error arise from neutron depolarization, half-wavelength contamination, multiple-scattering effects, and extinction. The magnetic properties of $Tb(OH)_3$ are highly anisotropic,[8] $g_{\parallel} = 18$ and $g_{\perp} = 0$, and we have applied the magnetic field parallel to the easy axis. Under these conditions neutron depolarization will be negligible. Half-wavelength contamination is especially serious at low temperature, when the magnetic-scattering amplitude is enhanced by the large moment at the terbium site. At 2.6 °K all measurements were taken with a ^{239}Pu filter in the incident beam; this reduces the contamination by a factor of 50. Multiple scattering and extinction are discussed further below.

A. Crystal structure

The rare-earth hydroxides have the hexagonal-yttrium-hydroxide structure.[16] The space group is $P6_3/m$ (No. 176) with two formula units in the unit cell. The unit cell dimensions of $Tb(OH)_3$ are $a = 6.270 \pm 0.005$ Å, and $c = 3.560 \pm 0.005$ Å. The atomic positions are 2 Tb in $(2d) \pm (\frac{2}{3}\ \frac{1}{3}\ \frac{1}{4})$, and both oxygen and hydrogen in

$$(6h) \pm (x\ y\ \tfrac{1}{4};\ -y\ x-y\ \tfrac{1}{4};\ y-x\ -x\ \tfrac{1}{4}).$$

The positions and thermal parameters of the oxygen and hydrogen atoms in the prototype structure $Y(OH)_3$ have been determined from x-ray and neutron-diffraction measurements by Christensen *et al.*[17] The projection of the structure onto the (00.1) plane is shown in Fig. 1.

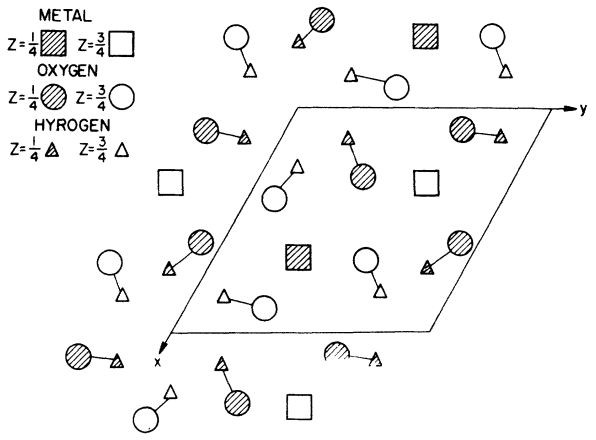

FIG. 1. (00.1) projection of the structure of $Tb(OH)_3$.

B. Multiple scattering

The presence of large extinction effects in the integrated intensities usually indicates that multiple scattering is also present.[18] To investigate the extent of any multiple scattering we have performed a number of azimuthal scans on nuclear peaks at room temperature. The most complete scans were those of the (00.2) and (00.3) reflections, and regions covering a 60° rotation about the scattering vector are shown in Fig. 2(a). The (00.2) is a strong reflection and no variation of this intensity is observed as the crystal is rotated about the azimuthal vector. Compare this, for example, with Fig. 5 of Moon and Shull,[18] in which sizeable variations in intensity occur when a similar experiment is performed on an iron crystal. The (00.3) reflection, on the other hand, has a structure factor of zero and should be more sensitive to multiple-scattering effects than the strong (00.2) reflection. However, the intensity of the (00.3) reflection is never significantly above the background level of ~75 counts for a full 60° rotation about the scattering vector. These scans, together with similar negative results obtained on the (11.0), (22.0), and (33.0) reflections, suggest that multiple scattering is negligible. Calculations with the Ewald sphere, which is broadened by the wavelength spread in the incident beam, and the reciprocal lattice of $Tb(OH)_3$ show that two points of the reciprocal lattice can be present simultaneously on the sphere. Visible proof of this process is provided in Fig. 2(b). In this experiment the crystal was set to diffract the (00.2) reflection on one side of the incident beam. By rotating about the scattering vector [keeping the (00.2) in the detector] the (13.$\bar{2}$) reciprocal-lattice point can be brought onto the Ewald sphere. Then, *without moving the crystal*, the detector was moved 100° (from +39 to −61°) to collect the (13.$\bar{2}$) reflection. The intensity as a function of the detector position is shown on the figure and demonstrates clearly that within the instrumental resolution simultaneous reflections exist in $Tb(OH)_3$, but the azimuthal scans in Fig. 2(a) show that the intensity of any one reflection is not significantly affected by this process.

C. Extinction

The initial refinements with the unpolarized-neutron data indicated that the structural parameters of $Tb(OH)_3$ are very close to those of $Y(OH)_3$. However, the refinements also showed that the crystal exhibited large extinction effects. These are described in detail in a separate publication,[19]

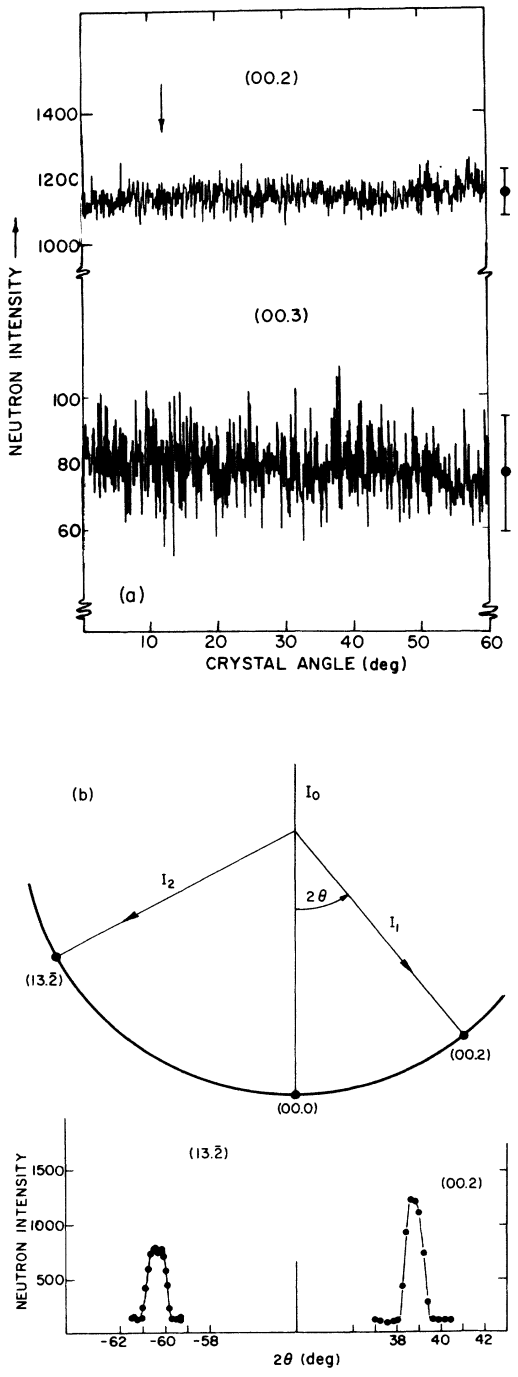

FIG. 2. (a) Experimental chart recording of azimuthal scans (i.e., rotation of the crystal about the scattering vector) for the (00.2) and (00.3) reflections of $Tb(OH)_3$ at room temperature. Counts were taken at 0.1° intervals. The error bars on the right hand side represent two standard deviations. The background at the (00.3) is ~75 counts. The arrow above the (00.2) scan indicates the crystal position for the simultaneous diffraction of the (13.$\bar{2}$) reflection. (b) The reciprocal-lattice construction for obtaining the (00.2) and (13.$\bar{2}$) reflections simultaneously.

but are outlined here briefly for completeness. With extinction the intensities of the strong Bragg intensities are reduced below the value expected from the kinematical theory. The most complete treatment of extinction has been given by Zachariasen.[20] For secondary extinction the Zachariasen formula may be written as

$$I_{obs}/I_c = y = 1/(1+2gQ\overline{T})^{1/2}\,, \tag{3}$$

where I_{obs} and I_c are the observed and calculated intensities, $\overline{T}$ is the effective path through the crystal, g is the extinction parameter, and Q is the crystallographic reflectivity given by $Q=\lambda^3|F_c|^2/(V^2\sin 2\theta)$. The calculated structure factor F_c includes any magnetic contribution; V is the volume of the unit cell and θ is the Bragg angle. For primary extinction $3Q\lambda^{-1}r^2$ is substituted for $2gQ\overline{T}$, where r is the radius of a perfect domain. The path lengths $\overline{T}$ for the present crystal, do not vary enough to distinguish between primary and secondary extinction. From the room-temperature data the atomic parameters were refined with a least-squares routine that included a correction for extinction of the form given in Eq. (3). The value of the residual ($=\sum||N_{obs}|-|N_c||/\sum|N_c|$, where N_{obs} and N_c are the observed and calculated nuclear-structure factors, respectively) immediately improved from the value of 0.189 without extinction corrections to 0.063. A further improvement to 0.036 was obtained by allowing anisotropic thermal vibrations. Both the metal and oxygen atoms showed little thermal anisotropy, in agreement with Ref. 17, but appreciable thermal anisotropy was observed for the hydrogen atom. The extinction parameter g was $(6\pm1)\times10^4$, and values of y [see Eq. (3)] were as low as 0.18. The large value of g for this crystal suggests that the extinction is either primary or secondary of type II. In both these cases the degree of extinction is not related to the mosaic spread of the crystal blocks. This characteristic of the extinction is demonstrated by the polarized-beam measurements in which the flipping ratio for a number of reflections has been measured as a function of the crystal-rocking angle. Figure 3 illustrates such measurements for the (10.0) reflection at 90 °K. The flipping ratio is independent of the intensity, and the mosaic character of the peak might suggest, incorrectly, that the extinction is not serious.

From Eq. (3) the observed flipping ratio

$$R_{obs}=\frac{I^+_{obs}}{I^-_{obs}}=\frac{I^+_c y^+}{I^-_c y^-}=R_{corr}\left(\frac{1+2gQ^-\overline{T}}{1+2gQ^+\overline{T}}\right)^{1/2}\,, \tag{4}$$

where superscripts refer to the two neutron spin states, and the terms Q^+ and Q^- contain the terms $(N+M)^2$ and $(N-M)^2$ substituted for F_c^2, respectively. The flipping ratio corrected for extinction is R_{corr}.

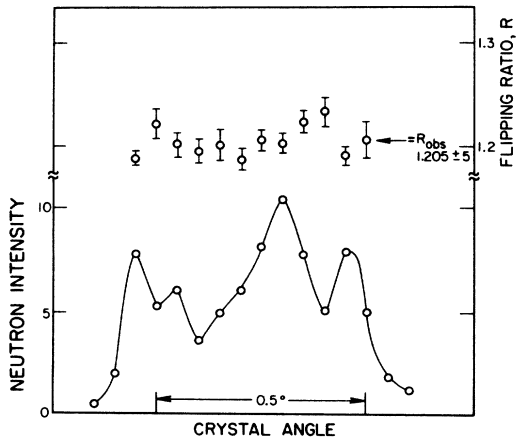

FIG. 3. Variation of the intensity and the flipping ratio R_{obs} as the crystal is rocked through the (10.0) reflection at 90°K with a field of 12 kOe applied parallel to the c axis.

The ratio of the magnetic to nuclear structure factors M/N can be obtained from a flipping ratio R, since

$$R = I^+/I^- = (N+M)^2/(N-M)^2 \ . \qquad (5)$$

Substituting R_{obs} or R_{corr}, in Eq. (5) leads to a determination of $(M/N)_{obs}$ or $(M/N)_{corr}$, respectively. With a knowledge of the nuclear structure factors N, the magnetic structure factors M_{obs}, or M_{corr}, may be obtained. Equations (4) and (5) have also to be modified for incomplete polarization and the spin-flipping efficiency, but, although these were considered in processing the data, they are omitted for the sake of clarity in this discussion.

The magnetic structure factor for a reflection $(hk.l)$ in $Tb(OH)_3$ is given by

$$M(hk.l) = 0.2696\ \mu f(\vec{\kappa})\, 2\cos 2\pi(\tfrac{2}{3}h + \tfrac{1}{3}k + \tfrac{1}{4}l) e^{-W} \times 10^{-12}\ \text{cm}, \qquad (6)$$

where μ is the magnetic moment per Tb atom, $f(\vec{\kappa})$ is the magnetic form factor, $\vec{\kappa}$ is the scattering vector, and $W = B_{Tb}\sin^2\theta/\lambda^2$ is the Debye-Waller factor for the terbium atom. The geometric factor reflects the fact that the terbium atoms are at the special positions $\pm(\frac{2}{3}\ \frac{1}{3}\ \frac{1}{4})$. We have used a value of 0.2 Å^2 for the isotropic temperature factor of terbium. Steinsvoll *et al.*[2] used 0.12 Å^2 for terbium metal at 4.2 °K. A value for the product of the moment and the form factor $(\mu f)_{obs}$ or $(\mu f)_{corr}$ after correcting for extinction may be obtained from M_{obs} or M_{corr}, respectively. To illustrate the extinction effects, we have plotted $(\mu f)_{obs}$ vs $\sin\theta/\lambda$ in Fig. 4 for the polarized-neutron data at 2.6°K as derived by substituting R_{obs} for R in Eq. (5). We expect the points to fall on, or near, the smooth curve. Clearly they do not, although the experimental uncertainties are often smaller than the points. This figure aptly demonstrates the importance of the extinction in this experiment.

D. Analysis

One approach to correct for extinction would be to use the values obtained for N and g from the unpolarized-neutron experiment and correct the polarized-neutron data. However, we have shown in Ref. 19 that it is possible to obtain the atomic parameters, as well as the magnetic structure factors and the magnitude of the extinction correction for each reflection, from the polarized-neutron data alone. This method relies on the fact that the values of M [see Eq. (6)] may be calculated using Hartree-Fock[5] (or other) form factors, and that the differences between the experimental and theoretical values of M are likely to be small.

The procedure adopted was as follows. First a theoretical magnetic form factor was assumed. This defines a set of $M(hk.0)$. Second an extinction parameter g was chosen, and Eq. (4) used to obtain a consistent set of M/N values corrected for extinction, $(M/N)_{corr}$. Since we have assumed a set of M, this defines a set of N_{corr}. These nuclear

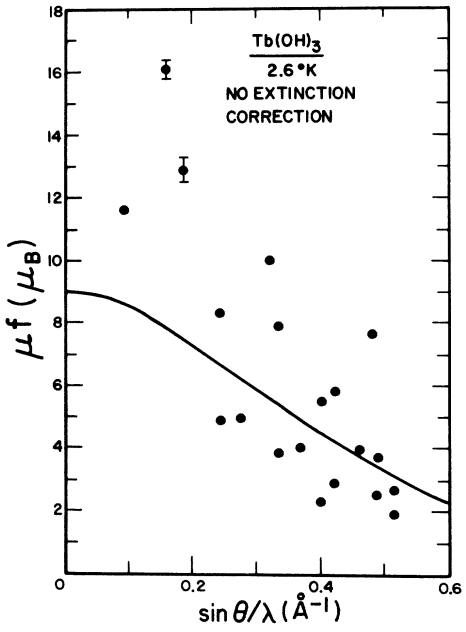

FIG. 4. Values of the product of the magnetic moment and the form factor $(\mu f)_{obs}$ derived from R_{obs} at 2.6°K with a knowledge of the atomic structure, but with no extinction correction. The smooth curve is the form factor for $Z = 2.52$ (see Sec. IV) normalized to $8.9\mu_B$/Tb atom. The experimental uncertainties are the size of the points unless otherwise indicated.

TABLE I. Measured flipping ratios R_{obs}, values of the product of the magnetic moment and the form factor corrected for extinction $(\mu f)_{corr}$, and calculated μf_c using $Z_4 = 2.52$ (see Sec. IV), for the polarized-neutron experiments at 90 and 2.6 °K. The errors refer to the least significant digit.

		90 °K			2.6 °K		
$(hk.l)$	$\sin\theta/\lambda$	R_{obs}	$(\mu f)_{corr}$	$\mu = 0.69\mu_B$ μf_c	R_{obs}	$(\mu f)_{corr}$	$\mu = 8.9\mu_B$ μf_c
10.0	0.092	1.205±5	0.651±14	0.659	16.0±2	8.58±5	8.55
11.0	0.159	4.190±40	0.623±16	0.604	1.427±9	8.33±13	7.85
20.0	0.184	•••	•••	•••	0.810±6	7.32±45	7.52
12.0	0.244	1.250±7	0.533±14	0.515	25.2±9	6.84±6	6.68
21.0		0.878±4	0.522±18	0.515	0.087±2	6.77±8	6.68
30.0	0.276	1.149±3	0.482±9	0.479	27.1±4	6.21±5	6.21
22.0	0.319	0.360±5	0.391±15	0.431	0.573±5	5.55±14	5.59
13.0	0.332	1.141±5	0.451±15	0.417	7.62±11	5.37±8	5.40
31.0		1.660±17	0.425±21	0.417	4.43±12	5.51±15	5.40
40.0	0.368	1.177±8	0.380±16	0.389	21.9±6	4.71±5	4.90
23.0	0.401	1.715±17	0.320±18	0.344	5.62±15	4.42±14	4.45
32.0		1.051±2	0.345±14	0.344	1.894±13	4.38±4	4.45
14.0	0.422	1.127±4	0.337±10	0.323	7.13±6	4.24±5	4.18
41.0		1.424±9	0.328±11	0.323	6.66±8	4.16±7	4.18
50.0	0.460	1.304±13	0.278±10	0.287	46.0±20	3.83±7	3.72
33.0	0.478	•••	•••	•••	1.243±6	4.01±45	3.51
24.0	0.487	0.886±5	0.264±12	0.264	0.150±4	3.32±7	3.41
42.0		•••	•••	•••	0.724±13	2.50±123	3.41
15.0	0.513	1.232±14	0.257±14	0.242	45.3±37	2.90±9	3.12
51.0		0.941±3	0.245±13	0.242	0.409±3	3.26±8	3.12

structure factors were then refined with a conventional least-squares routine. This procedure was followed for three different form factors (discussed below), but the atomic parameters obtained were found to be independent of the initial magnetic form factor chosen. For data at both 90 and 2.6 °K, the best fit for all assumed magnetic form factors was with an extinction parameter $g = 5\times10^4$. This value is in agreement with the $g = (6\pm1)\times10^4$ deduced from the room-temperature study with unpolarized neutrons. The structural parameters deduced from these refinements (tabulated in Ref. 19) were essentially unchanged from those at room temperature, except for a small increase in the thermal anisotropy of the hydrogen atom. The residuals of these refinements were in the range of 0.02, indicating that the Zachariasen formula is very successful in accounting for the extinction. As a final step, the structural parameters were used to calculate the nuclear structure factors and R_{obs} reprocessed to obtain M_{corr}, and hence $(\mu f)_{corr}$. The values of R_{obs}, $(\mu f)_{corr}$, and calculated μf_c values (see Sec. IV) are given for both temperatures in Table I. The errors on R_{obs} in Table I are derived from the uncertainties in the instrumental parameters and from counting statistics. The errors on $(\mu f)_{corr}$ have been determined by varying R_{obs} as well as the structural and extinction parameters within their experimental uncertainties. The squares of the inverse of the errors on $(\mu f)_{corr}$ are used as relative weights in the analysis below. The very large errors on $(\mu f)_{corr}$ for the weak reflections (200), (330), and (420), stem from the sensitivity of these reflections to the exact position of the oxygen and hydrogen atoms. Since we are interested in determining the magnetic form factor, these reflections carry very small weights in the subsequent analysis.

E. Covalency

The problem of covalency in transition-metal compounds has received much attention.[21,22] In the rare-earth series relatively little work has been done on this subject, although calculations by Baker[23] and Byrom *et al.*[24] show that the effects may be important. The exchange interaction between neighboring magnetic ions in transition-group salts is closely related to covalency. In the rare-earth hydroxides the exchange interactions are almost completely dipolar in origin and we therefore anticipate the covalency to be negligible in these materials. In a ferromagnetic or paramagnet covalency can cause a net spin density to be located at sites other than the magnetic ion. In the $Tb(OH)_3$ structure, the positions of any such spin densities might be expected to be located on the terbium–$(OH)^-$ bond; i.e., at positions of $6h$, or lower, symmetry. An examination of Eq. (6) shows that reflections with $(hk.l)$ where l is odd and $h-k = 3n$ (n integer) have no contribution from

TABLE II. Flipping ratios at 90 °K for reflections that have no contribution from the terbium atom. q^2 is the square of the magnetic interaction vector. At $T=2.6$ °K, R_{obs} for the (11.1) reflection is 0.993 ± 3.

$(hk.l)$	$\sin\theta/\lambda$	q^2	R_{obs}
11.1	0.213	0.563	0.999 ± 4
30.1	0.310	0.795	1.001 ± 7
14.1	0.445	0.800	1.004 ± 7
41.1			1.002 ± 8
33.1	0.499	0.921	1.001 ± 6

the terbium atoms. These reflections, however, have contributions from any atom or magnetization density located at positions of $6h$, or lower, symmetry. The important point is that any spin density not having the exact translational symmetry of the terbium atom (for example, if the spin density is associated with the metal to ligand bond) will contribute to the flipping ratio of these special reflections. The examination of these reflections is analogous to polarized-neutron experiments[25] on MnF_2. Such reflections cannot, of course, be measured in the basal $(hk.0)$ plane, but may be examined easily with the elevated-counter technique. The results are given in Table II and in no case is the deviation from unity significant. In particular, the (11.1) reflection arises almost entirely from oxygen scattering, and the observed flipping ratios at 90 and 2.6 °K indicate that any moment located at the oxygen site must be less than $0.01\mu_B$. As a final remark we note that Table II also strengthens our statements that multiple scattering is probably negligible in this experiment. These reflections are surrounded in reciprocal space by reflections with $R \neq 1$, and any double-scattering processes would almost certainly result in measurable values for $|R-1|$ at these special Bragg positions.

IV. WAVE FUNCTIONS

The theoretical form factors calculated from Eq. (2) require an evaluation of the $\langle j_i \rangle$ integrals which depend on the spatial extent of the single-electron $4f$ wave function. The $\langle j_i \rangle$ integrals derived from the nonrelativistic wave functions of Freeman and Watson[5] (FW) have been tabulated by Blume *et al.*[26] and used frequently in calculating neutron magnetic form factors. FW used a linear combination of four hydrogenic orbitals as a basis set for the radial part of the $4f$ electron wave function. The radial part of the wave function is given by

$$U_{4f}(r) = \sum_{i=1}^{4} C_i r^4 e^{-Z_i r} , \tag{7}$$

where the normalization condition is

$$\int_0^\infty U_{4f}^2(r)\, dr = 1 .$$

The coefficients C_i and Z_i are given in Table I of FW, and the $\langle j_i \rangle$ integrals obtained from

$$\langle j_i \rangle = \int_0^\infty U_{4f}^2(r)\, j_i(\kappa r)\, dr , \tag{8}$$

where $j_i(\kappa r)$ is the usual spherical Bessel function.

As discussed in Sec. I, the experimental results for the rare-earth metals[1-4] indicate that the spatial extent of the $4f$ electrons is more expanded in real space than given by the FW wave functions. This expansion must be described quantitatively if the experimental form factors of terbium metal and terbium in $Tb(OH)_3$ are to be compared both with each other and with theory. We have used the method of varying the coefficients C_i and Z_i for the hydrogenic orbitals in Eq. (7). A complete discussion of this process is given in Ref. 7, and will not be repeated here. Two points are important in this fitting procedure. First, the experimental rare-earth form factors can be reproduced very well by varying Z_4 only, keeping the remaining Z_i's and the ratios between the C_i coefficients the same as in the FW expansion. Second, to define Z_4 uniquely, the value of the $4f$ moment must be known. For terbium metal, the low-angle data of Ref. 2 suffer from extinction, but we have fitted the high-angle data of Ref. 2 and the data of Ref. 3 with the same value[27] of $Z_4 = 2.36$. The FW value of Z_4 is 2.67. In these analyses we assume that the $4f$ moment is $9.0\mu_B$/Tb atom in the ordered state,[2] and that the total induced moment in the paramagnetic regime[3] is $4f$ in nature. Since the exact contribution of the conduction electrons to the total magnetic moment measured in magnetization experiments[28] is not known experimentally, the form factor determined for terbium metal depends on the validity of the assumptions outlined above.

In ionic $Tb(OH)_3$ no discrepancy between the expected $4f$ moment and the experimental value[8] is observed, and the question of conduction-electron polarization does not arise. Following Ref. 7 we have obtained the best fit for a given magnetic form factor to the experimental data of $Tb(OH)_3$, with the magnetic moment as a parameter. A measure of the goodness of the fit is the quantity s, defined by

$$s = \left(\sum_i W_i \left[(\mu f)_{corr} - \mu f_c \right]_i^2 \right) \Big/ n , \tag{9}$$

where $W_i = 1/\Delta\mu f_{corr}{}^2$, and the sum is over all reflections. The results for three values of Z_4 are given in Table III and illustrated in Figs. 5 and 6. The lowest value of s with μ as a parameter is obtained for $Z_4 = 2.52$. These analyses may be visualized simply as fitting a straight line through

TABLE III. Values of Z_4 and the magnetic moment per Tb atom (in Bohr magnetons) that give the best fit, as measured by the minimum of s in Eq. (9), between the experimental and theoretical form factors. The last row gives the values of s for a fixed value of $\mu = 8.9\mu_B$.

		FW	Metal	Best fit
	Z_4	2.67	2.36	2.52
90 °K	μ	0.67 ± 0.01	0.74 ± 0.01	0.69 ± 0.01
	s	1.4	2.2	1.3
2.6 °K	μ	8.68 ± 0.04	9.48 ± 0.04	8.95 ± 0.03
	s	6.2	5.9	2.9
2.6 °K	μ	8.90	8.90	8.90
	s	10.0	27.8	3.2

a plot of $(\mu f)_{corr}$ against f_c and we present such a plot for $Z_4 = 2.52$ in Fig. 7. For all three values (2.67, 2.52, and 2.36) of Z_4 a straight line may be drawn through the points and the origin [i.e., $f_c = (\mu f)_{corr} = 0$]. The parameter s of Eq. (9) is a measure of the spread of points about this straight line. Ideally, if the scatter of points is comparable to the experimental standard deviations then $s \simeq 1$. The somewhat larger values of s are an indication of possible systematic errors in the analysis. If the weights in Eq. (9) are regarded as relative only, the standard error on μ (the intercept with $f_c = 1$ in Fig. 7) is defined as $(s/\Sigma W_i)^{1/2}$. The values of s, μ and the errors on μ are given in

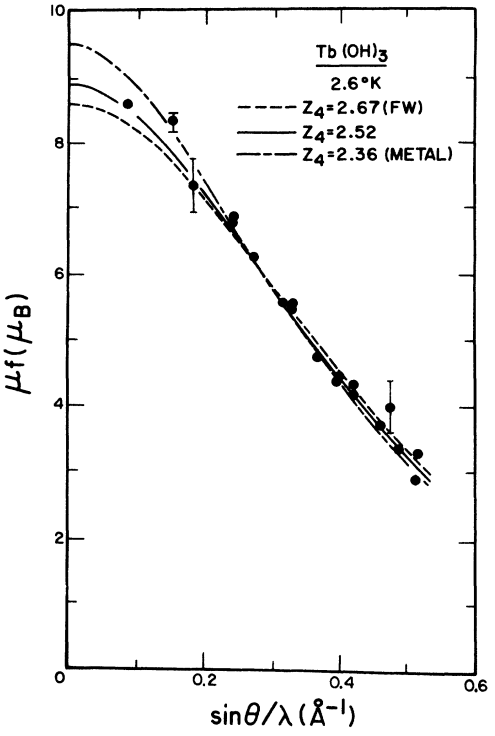

FIG. 6. Values of $(\mu f)_{corr}$ derived from R_{corr} at 2.6 °K with an extinction parameter of $g = 5 \times 10^4$. The smooth curves are as in Fig. 4, normalized to the moment values given in Table III. The experimental uncertainties are the size of the points unless otherwise indicated.

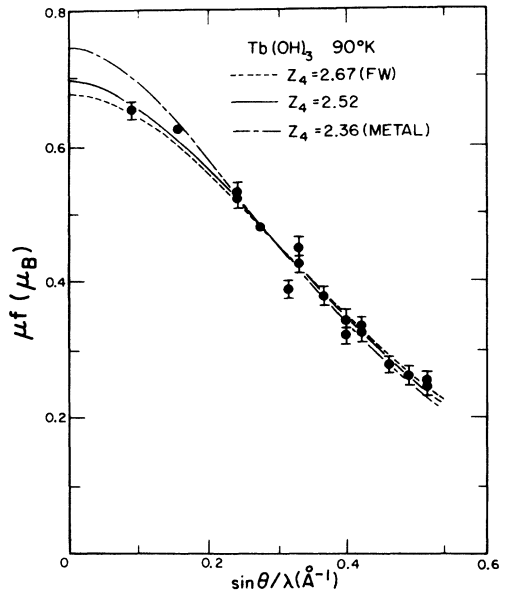

FIG. 5. Values of $(\mu f)_{corr}$ derived from R_{corr} at 90 °K with an extinction parameter of $g = 5 \times 10^4$. The smooth curves are various magnetic form factors adjusted to give the best fit to the experimental points (see Sec. IV).

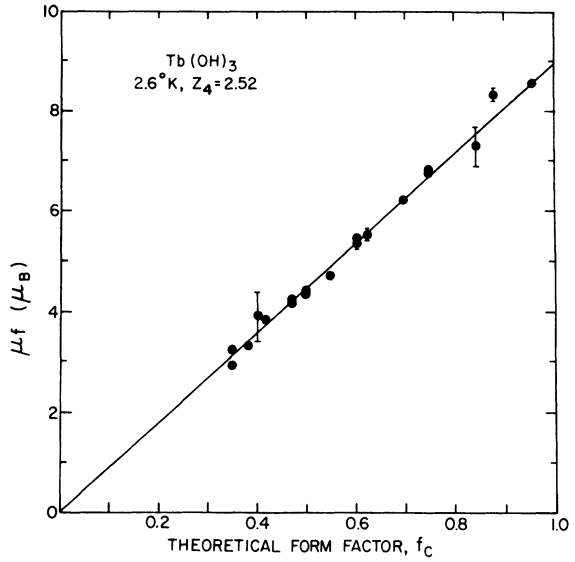

FIG. 7. Values of $(\mu f)_{corr}$ from the 2.6 °K data plotted vs f_c derived with $Z_4 = 2.52$. The straight line is the least-squares fit through the data and the origin.

Table III. At 90 °K the experimental magnetic moment is 0.67 ± 0.03 μ_B per Tb atom (see Sec. II). The use of the metal form factor gives an unacceptable value of $0.74 \pm 0.01 \mu_B$, but the FW and $Z_4 = 2.52$ (best fit) form factors cannot be distinguished. At 2.6 °K, however, the experimental moment is $(8.90 \pm 0.05) \mu_B$, and both the FW and metal form factors are clearly excluded because their values of μ are more than three standard deviations from the correct value. Another way to illustrate the lack of agreement with the FW and metal form factors is to evaluate s with the magnetic moment fixed at the correct value of $8.90 \mu_B$. The results are given in the last row of Table III. The improvement in s from 10.0 (or from 27.8 in the case of the metal form factor) to 3.2 is significant.

The radial integrals $\langle j_0 \rangle$ and $\langle j_2 \rangle$ used to calculate the magnetic form factors are given for the three values of Z_4 in Table IV.

In the initial analysis of R_{obs} in Sec. III, the only values of Z_4 used were 2.67 (FW) and 2.36 (metal); both leading to the same set of atomic parameters, and thus the same set of $(\mu f)_{corr}$. As discussed above, the best fit obtained to this set of $(\mu f)_{corr}$ is with $Z_4 = 2.52$. A new set of N_{corr} was derived with this value of Z_4. For this set we obtained a lower value of the crystallographic residual (see Sec. III) than with the two other sets of N_{corr}; illustrating the consistency of the procedure.

Finally, a cursory inspection of Figs. 5 and 6 might suggest that the determination of the experimental form factor depends heavily on the first three reflections. This is not the case, however; indeed, if these first three reflections are omitted from the analysis the changes in the entries in Table III are insignificant. The reason for this is that our analysis essentially determines an experimental value of μ for each reflection by implicitly performing the operation $\mu = (\mu f)_{corr}/f_c$. The absence of any conduction-electron polarization then allows the value of μ to be compared with theory and magnetization experiments.

TABLE IV. Values of $\langle j_0 \rangle$ and $\langle j_2 \rangle$ for different Z_4 values for terbium. The best experimental fit is with $Z_4 = 2.52$.

	$Z_4 = 2.67$ Freeman and Watson (Ref. 5)		$Z_4 = 2.36$ Metal form factor		$Z_4 = 2.52$	
	$\langle j_0 \rangle$	$\langle j_2 \rangle$	$\langle j_0 \rangle$	$\langle j_2 \rangle$	$\langle j_0 \rangle$	$\langle j_2 \rangle$
0	1	0	1	0	1	0
0.10	0.946	0.021	0.925	0.029	0.939	0.024
0.20	0.809	0.072	0.751	0.089	0.788	0.078
0.30	0.635	0.127	0.562	0.139	0.608	0.132
0.40	0.464	0.169	0.399	0.169	0.439	0.170
0.50	0.317	0.194	0.268	0.181	0.298	0.189
0.60	0.202	0.200	0.169	0.181	0.190	0.193
0.70	0.118	0.193	0.097	0.171	0.110	0.184
0.80	0.060	0.177	0.048	0.155	0.056	0.168

V. CONCLUSIONS

The magnetic form factor in $Tb(OH)_3$ has been measured with polarized neutrons at 90 and 2.6 °K. The experimental results suffer from severe extinction effects, but, perhaps surprisingly, the Zachariasen[20] formula is totally adequate in correcting the data. This aspect of the experiment is discussed in greater detail in a companion publication.[19] The extent of the extinction corrections may be seen by comparing the uncorrected points of Fig. 4 with the corrected points of Fig. 6. The discrepancies between $(\mu f)_{corr}$ and μf_c in Table I may indicate some subtleties in the atomic structure, inadequacies in the extinction formula, or both. Any further examination of these effects should be done on crystals exhibiting less extinction.

We have found no evidence for covalency in $Tb(OH)_3$. Deviations of the experimental points from the smooth form-factor curve are discussed above, and without further experiments, should not be attributed to asphericities in the magnetization density. In a separate experiment, we have searched for, and not found, any evidence for a small transferred spin located away from the magnetic ion.

The magnetic form factor of terbium in $Tb(OH)_3$ is in excellent agreement with recent relativistic calculations.[29] In gadolinium metal the experimental magnetic form factor[1] is also in good agreement with relativistic calculations.[6] The disagreement between the Tb^{3+} form factor in $Tb(OH)_3$ (or the relativistic form factor) and that for terbium metal is not understood; but the interpretation of the metal form factor could be in error due to the invalidity of the assumptions regarding the $4f$ moment. In those ionic systems with well-understood magnetic properties, experiments to determine the magnetic form factor of the rare-earth ion, and the extent of covalency, would be of interest. In truly ionic systems the conduction-electron polarization is absent, and a free-ion form factor may be obtained experimentally, as we have done in $Tb(OH)_3$. The free-ion form factors may then be compared both with those derived theoretically and with those measured for the metals.

ACKNOWLEDGMENTS

We would like to thank W. P. Wolf for the loan for the crystals and helpful conversations concerning the magnetic properties of $Tb(OH)_3$. We have benefited from many discussions with A. J. Freeman.

†Work performed under the auspices of the U. S. Atomic Energy Commission.

[1]R. M. Moon, W. C. Koehler, J. W. Cable, and H. R. Child, Phys. Rev. B 5, 997 (1972).
[2]O. Steinsvoll, G. Shirane, R. Nathans, M. Blume, H. A. Alperin, and S. J. Pickart, Phys. Rev. 161, 499 (1967).
[3]T. O. Brun and G. H. Lander, J. Phys. (Paris) 32, C1-571 (1971).
[4]T. O. Brun and G. H. Lander, Phys. Rev. Lett. 23, 1295 (1969).
[5]A. J. Freeman and R. E. Watson, Phys. Rev. 127, 2058 (1962).
[6]A. J. Freeman and J. P. Desclaux, Int. J. Magn. 3, 311 (1972).
[7]G. H. Lander, T. O. Brun, and O. Vogt, Phys. Rev. B 7, 1988 (1973).
[8]W. P. Wolf, H. E. Meissner, and C. A. Catanese, J. Appl. Phys. 39, 1134 (1968).
[9]P. D. Scott and W. P. Wolf, J. Appl. Phys. 40, 1031 (1969).
[10]A. T. Skjeltorp and W. P. Wolf, J. Appl. Phys. 42, 1487 (1971).
[11]P. D. Scott, thesis (Yale University, 1970) (unpublished).
[12]P. D. Scott, H. E. Meissner, and H. M. Crosswhite, Phys. Lett. A 28, 489 (1969).
[13]S. W. Lovesey and D. E. Rimmer, Rep. Prog. Phys. (London) 32, 333 (1969).
[14]G. H. Lander and T. O. Brun, J. Chem. Phys. 53, 1387 (1970).
[15]S. Mroczkowski, J. Eckhart, H. E. Meissner, and J. C. Doran, J. Crys. Growth 7, 333 (1970).
[16]R. W. G. Wyckoff, in *Crystal Structures* (Interscience, 1964), Vol. II, p. 77.
[17]A. N. Christensen, R. G. Hazell, and A. Nilsson, Acta Chem. Scand. 21, 481 (1967).
[18]R. M. Moon and C. G. Shull, Acta Crystallogr. 17, 805 (1964).
[19]G. H. Lander and T. O. Brun, Acta. Crystallogr. A 29, 684 (1973).
[20]W. H. Zachariasen, Acta Crystallogr. 23, 558 (1967).
[21]J. Owens and J. H. M. Thornley, Rep. Prog. Phys. (London) 29, 675 (1966), and references therein.
[22]W. Marshall and S. W. Lovesey, *Theory of Thermal Neutron Scattering* (Oxford U. P., Oxford, England, 1971), p. 209.
[23]J. M. Baker, J. Phys. C 1, 1670 (1968).
[24]E. Byrom, D. E. Ellis, and A. J. Freeman, AIP Conf. Proc. 10, 1294 (1973).
[25]R. Nathans, H. A. Alperin, S. J. Pickart, and P. J. Brown, J. Appl. Phys. 34, 1182 (1963).
[26]M. Blume, A. J. Freeman, and R. E. Watson, J. Chem. Phys. 37, 1245 (1962); J. Chem. Phys. 41, 1878 (1964).
[27]T. O. Brun, G. H. Lander, and G. P. Felcher, Bull. Am. Phys. Soc. 16, 325 (1971).
[28]D. E. Hegland, S. Legvold, and F. H. Spedding, Phys. Rev. 131, 158 (1963).
[29]G. H. Lander, T. O. Brun, J. P. Desclaux, and A. J. Freeman, Phys. Rev. B 8, 3237 (1973).